Thermoreversible Gelation of Poly(vinylidene flouride) in Diethyl Adipate: A Concerted Mechanism

Asok K. Dikshit and Arun K. Nandi*

Polymer Science Unit, Indian Association for the Cultivation of Science, Jadavpur, Calcutta 700 032, India

Received May 13, 1998

ABSTRACT: Poly(vinylidene flouride) (PVF_2) gels in diethyl adipate (DEA) with fibrillar morphology. The gels are transparent. The Wide-angle X-ray scattering pattern and FT-IR spectra of the gel indicate the presence of solvated α-phase PVF_2 crystallites in the gel. The intensities of the X-ray diffraction peaks of the gel are mostly different than those of the melt-crystallized sample. The plots of enthalpy of gel fusion and enthalpy of gel formation with a weight fraction of PVF_2 (W_{PVF_2}) indicate a positive deviation from linearity. Analysis of these results indicates polymer−solvent complex formation in the molar ratio of 1:2 for the DEA and PVF_2 repeating unit, respectively. The phase diagram also supports polymer−solvent complex formation with an incongruent melting point. The gelation kinetics is studied by the test tube tilting method. Analysis of the concentration function of the gelation rate supports the theory that this gelation process obeys the three-dimensional percolation mechanism. The temperature coefficient analysis is done both by the Flory and Weaver theory of coil-to-helix transtion and by the growth rate theory of fibrillar crystallization extended to the polymer−diluent system. A comparison of energy barrier values of both the processes indicates that the gelation is a concerted process of conformational ordering and crystallization.

Introduction

Thermoreversible gelation of poly(vinylidene fluoride) (PVF_2) has gained considerable interest[1−5] because of its possible use as a polymer gel actuator (semirigid transducer). In the thermoreversible gelation of PVF_2, usually crystallites act as junction points. PVF_2 can crystallize in five different polymorphs (e.g., α, β, γ, δ, and ϵ), of these only the α-polymorph is produced under normal crystallization conditions.[6]

The thermoreversible PVF_2 gels reported so far have mainly spheroidal morphology.[1−3] Only very recently, we reported a PVF_2 gel where the morphology is fibrillar.[5] It is now pointed out by some authors[7] that thermoreversible gels with spheoridal morphology do not have adequate elastic property while the fibrillar gels have a good elastic property. In our earlier report we observed that PVF_2 gels in glyceryl tributyrate (GTB) have fibrillar morphology,[5] so it is interesting to have fibrillar gels of PVF_2 in other systems also to understand the molecular mechanism of gelation in these systems.

In this paper we shall draw attention mainly on the structure and morphology of the gel. An attempt will be made from the thermodynamic study of the gels to understand the cause of formation of the fibrillar morphology in this system. The kinetic study of the gelation process will be done to understand the gelation mechanism both from a macroscopic and microscopic viewpoint. Thus, from both the thermodynamic and kinetic study we shall try to understand the mechanism of formation of a fibrillar PVF_2 gel.

Experimental Section

Samples. A commercial PVF_2 sample (ky-201, Pennwalt Corp.,United States) is used in the work. The sample is recrystallized from its dilute solution in acetophenone, washed with methanol, and dried in a vacuum at 60 °C for 3 days. The polymer has a weight-average molecular weight ($\bar{M}_w$) = 8.81×10^5, polydispersity index = 2.82, and head-to-head (H−H) defect = 5.31 mol %.[2] The solvent diethyl adipate (DEA) is purchased from Lancaster and is used as received.

Preparation of Gel and Its Characterization. The gels are prepared in two ways. For morphology, structural, and kinetic investigation they are made in glass tubes and for thermodynamic study they are made in Perkin-Elmer LVC capsules. In the first method an appropriate amount of polymer and solvent is taken in a glass tube, degassed by the freeze−thaw technique, and sealed under vacuum (10^{-3} mmHg). They are made homogeneous at 180 °C and quickly gelled by quenching at different temperatures. For SEM (scanning electron microscopy) study the gels, prepared at 30 °C, are taken out from the sealed tubes and dried at 35 °C under vacuum for 3 days. They are then gold-coated and their micrographs are taken in a SEM apparatus (Hitachi S-415A). The TEM (transmission electron microscopy) study of the gel is done by dropping a 1% solution of PVF_2 in DEA directly on a carbon-coated copper grid and then dried at 35 °C in a vacuum. The gel is then observed in the electron microscope (Hitachi H-600). For the WAXS study of dried gel (dried in a vacuum at 35 °C for 1 month) a Phillips powder diffraction apparatus (model PW1710) is used with nickel-filtered Cu Kα radiation. The gel is taken in a glass groove and the diffractogram of the gel is recorded at the scanning rate of 0.09° 2θ/min. For FT-IR study a Nicolet FT-IR instrument [Magna-IR 750 spectrometer (series-II)] is used. The solvent spectra are subtracted from the gel spectra to get the PVF_2 spectra in a gel form using the computer attached to the instrument.

Thermodynamic Study. Thermodynamic study of gelation is done using a differential scanning calorimeter (DSC-7, Perkin−Elmer). The required amount of polymer and solvent with varying compositions are taken in the Perkin-Elmer LVC capsules and are tightly sealed with the help of a quick press. They are made homogeneous by melting at 180 °C with occasional shaking for 10 min. They are then quenched to 20 °C in a DSC, and after equilibrating for 20 min they are heated at the rate of 40 °C/min. The higher heating rate is chosen to avoid melt recrystallization during the heating process.[5,8] The peak temperature has been taken as the gel-melting temperature. From the area of the peak the enthalpy of gel fusion is

10.1021/ma980764n CCC: $15.00
Published on Web 11/25/1998

measured. The DSC is calibrated with indium before each set of experiments.

The enthalpies of gelation and the gel formation temperature are measured in DSC by the dynamic cooling method. The LVC capsules containing homogeneous solution at 180 °C are cooled at the rate of 5 °C/min from that temperature to 20 °C and the exotherms are recorded. From the peak temperature and the peak area, the gel formation temperature and the enthalpy of gelation are measured.

The equilibrium gel melting (T^0_{gm}) and the equilibrium dissolution temperature(T^0_d) are measured using the Hoffman−Weeks procedure.[9] After being kept at 180 °C, the above DSC capsules are quenched to the desired isothermal gelation temperature and are kept for a definite time (3 h) for each case. The instrument is then scanned at the rate of 10 °C/min from that temperature to 180 °C. The peak temperature is taken as the gel-melting temperature.[5] The dissolution temperatures are obtained by crystallizing the LVC capsules above 60 °C for 12 h at each temperature. The instrument is then scanned as above.

Kinetic Study. The kinetics of gelation is studied by the test tube tilting method.[1−5,10−12] To make gels at different polymer concentrations, 0.5 mL of diethyl adipate (density = 1.009 g/mL) and an appropriate amount of PVF_2 (5−60 mg) are taken in glass tubes (8-mm i.d. and 1-mm thick). They are degassed by the freeze−thaw technique and are sealed under vacuum (10^{-3} mmHg). They are made homogeneous at 180 °C and are quickly transferred to a thermostatic bath set at a predetermined temperature. The gelation time (t_{gel}) is counted as the time where no flow occurs after the tube is tilted. The perfection in the rate measurement has been reached up to (t_{gel}) = ±5 s by a trial and error procedure.

Results and Discussion

Morphology and Structure. The PVF_2 gels in diethyl adipate are colorless and transparent materials. The scanning electron micrograph and transmission electron micrograph of dried PVF_2 gel in DEA are presented in Figure 1. From both the micrographs it is clear that the dried gel consists of fibrils which constitute the network structure. Of course, it is necessary to maintain here that it has been assumed throughout the paper that the PVF_2 gel in the undried state also has a similar morphology. In Figure 2 the WAXS pattern of dried gel is presented and it corresponds to that of the α-polymorph.[13−16] The d_{hkl} values are calculated from the Bragg equation and are presented in Table 1. The experimental d values tally excellently with the calculated d values using a pseudo-orthorhombic unit cell. In the last two columns of the table the relative intensities of the diffraction peaks are compared with respect to its 110 peak for both the melt-crystallized PVF_2 and also for the PVF_2 gel. A comparison of the intensity ratios of the two columns indicate that except in a few cases the intensity ratios do not match each other. This result indicates that though the crystal system and the d spacing remain the same, the atomic positions of the statistical up-and-down arrangment of the chains in the unit cell may be somewhat changed. This may be due to the orientation effect of the solvent during gelation and will be discussed later. However, we are unable to assign here the diffraction peaks at $2\theta = 16.9$, 22.6, and 24.0 with the literature value,[13−15] and it may be argued that these peaks are newly observed in the gel form of PVF_2.

The crystalline polymorph involved in the gel formation is also ascertained by FT-IR spectra of the gel. It has been done to understand if any change in the polymorphic structure occurs during drying. The solvent-subtracted FT-IR spectra of the gel are shown in Figure 3. This figure clearly indicates the presence of α-crystallites in the gel because the peak at 532 cm^{-1} corresponds to that of the α-polymorph only with TGTḠ conformation.[17−20] The other peaks tally excellently with those of the α-PVF_2 except the two shoulders at 640 and 589 cm^{-1}. The reason for the appearance of these two shoulders is not yet known. Thus, it may be concluded that during the drying of the gel in a vacuum at room temperature (35 °C) no change in the polymorphic structure occurs. However, the new diffraction peaks in the X-ray pattern may be due to the solvated structure of the α-form crystals of PVF_2.[21,22]

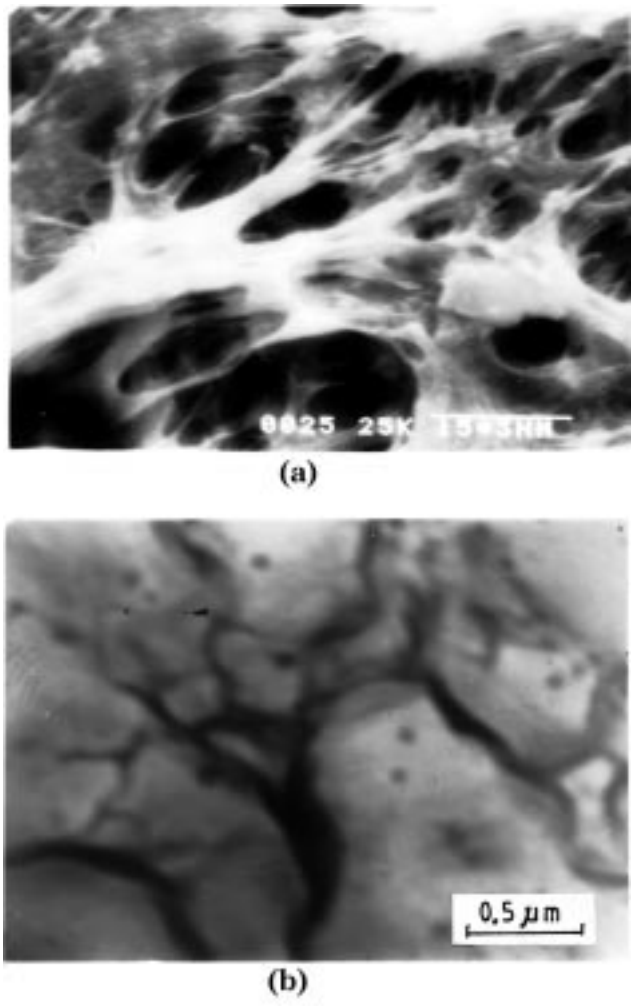

Figure 1. (a) The scanning electron micrograph of dried PVF_2 gel (6 g/dL) in diethyl adipate prepared at 30 °C. (b) The transmission electron micrograph of dried PVF_2 gel (1 g/dL) in diethyl adipate prepared at 30 °C.

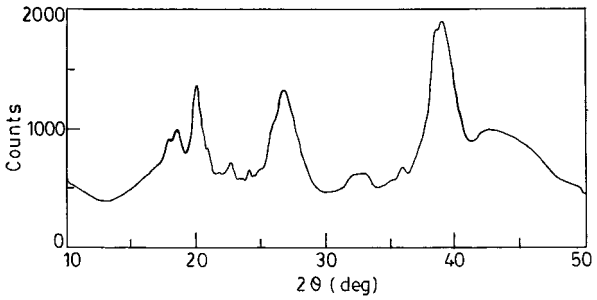

Figure 2. The WAXS pattern of dried PVF_2 gel (6 g/dL) in diethyl adipate prepared at 30 °C.

Thermodynamics of Gelation. In Figure 4a,b the representative thermograms of the PVF_2 gels in diethyl

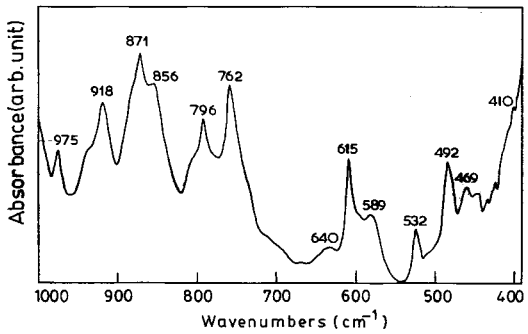

Figure 3. Solvent-subtracted FT-IR spectra of PVF_2 gel (6 g/dL) in diethyl adipate prepared at 30 °C.

Table 1. X-ray Data of PVF_2–DEA Gel [d_{hkl} (Calculated) for α-Phase PVF_2 with a = 5.02 Å, b = 9.63 Å, and c = 4.62 Å and I^0_{hkl} = Observed Intensity]

hkl	d_{hkl} (calculated)	d_{hkl} (observed)	I^0_{hkl}/I^0_{110} melt crystal[14,15]	I^0_{hkl}/I^0_{110} (gel)
		5.24		0.34
100	5.02	4.97	0.52	0.52
020	4.81	4.82	0.64	0.58
110	4.45	4.43	1.0	1.00
011	4.17	4.20	0.17	0.33
		3.93		0.23
		3.70		0.14
021/101	3.33	3.35	0.70	0.91
121	2.79	2.79	0.41	0.17
130	2.70	2.69	0.48	0.17
200	2.51	2.50	0.54	0.16
131	2.33	2.34	0.52	1.40
002	2.31	2.31		1.44
211/041	2.15	2.13	0.51	0.25
230	1.98	1.98	0.19	0.21

adipate produced at different conditions are presented. In all cases a single melting peak/gelation peak is observed. In Figure 5 the gel-melting enthalpies and gel formation enthalpies are plotted for the whole composition range of PVF_2 in the gel. It is apparent from the figure that there is a positive deviation from linearity from the line joining those of the pure components. The enthalpy of gel melting or enthalpy of gel formation (ΔH) may be considered to consist of three terms:

$$\Delta H(\text{per g}) = w_1\Delta H_1 + w_2\Delta H_2 + \Delta H_c \qquad (1)$$

where w represents the weight fraction, subscripts 1 and 2 represent the solvent and the polymer, respectively, ΔH_1 and ΔH_2 are the melting or crystallization enthalpies of the solvent and polymer, respectively, and ΔH_c arises due to the formation of any organized structure (e.g., polymer–solvent compound formation) in the gel. In the present case of interest the contribution of the first term is zero since the solvent does not crystallize at the temperature of interest. So

$$\Delta H - w_2\,\Delta H_2 = \Delta H_c \qquad (2)$$

The left-hand side (lhs) of eq 2 corresponds to the positive deviation (Δ) from linearity in Figure 5.

In Figure 6, the deviation (Δ) is plotted with w_{PVF_2} and there is a maximum in the plot. This indicates that there is a polymer–solvent complex formation in the system.[23] In analogy with Tamman's plot the maximum indicates the composition of a polymer–solvent complex formation.[24–27] The stoichiometry of the complex calculated from the composition of the maximum is equal

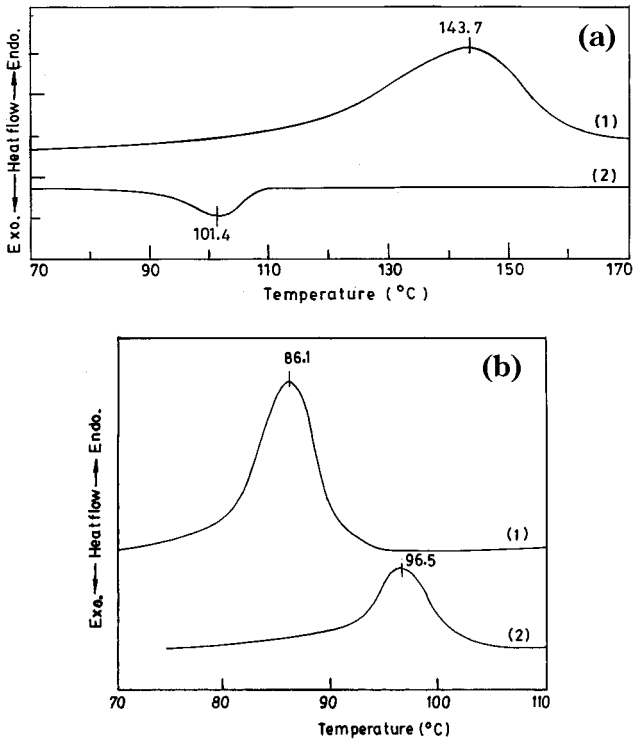

Figure 4. (a) Representative DSC thermograms of the PVF_2 gel (W_{PVF_2} = 0.54) in diethyl adipate: (1) gelled at 20 °C for 20 min and scanned at 40 °C/min. (2) Cooled from 180 °C at 5 °C/min. (b) Representative DSC thermograms of the PVF_2 gel (7.2 g/dL) in diethyl adipate (1) gelled at 40 °C for 3 h and scanned at the heating rate 10 °C/min. for (T^0_{gm}). (2) Crystallized at 65 °C for 12 h and scanned at 10 °C/min (for T^0_d).

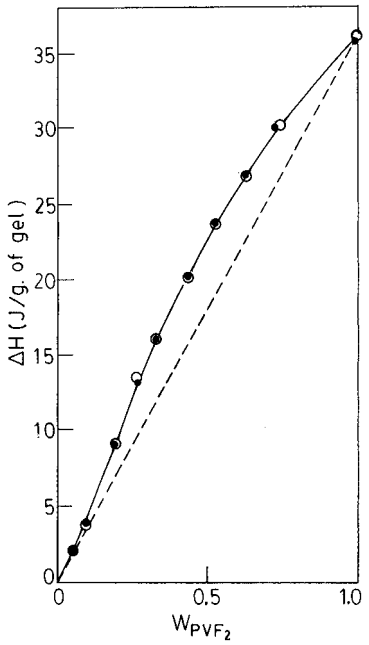

Figure 5. Enthalpy changes during the gel-melting/gelation process of PVF_2/diethyl adipate gels vs the w_{PVF_2} plot: ○, melting; ●, gelation.

to w_{PVF_2} = 0.39. This corresponds to a 1:2 complex formation in the molar ratio of DEA and PVF_2 repeating unit, respectively. Since >C=0 group have some specific interaction with $>CF_2$ dipoles of PVF_2, it may be presumed that the compound formation is occurring through the dipole–dipole interaction of the above two groups.[20,28] However, the detailed structure of the

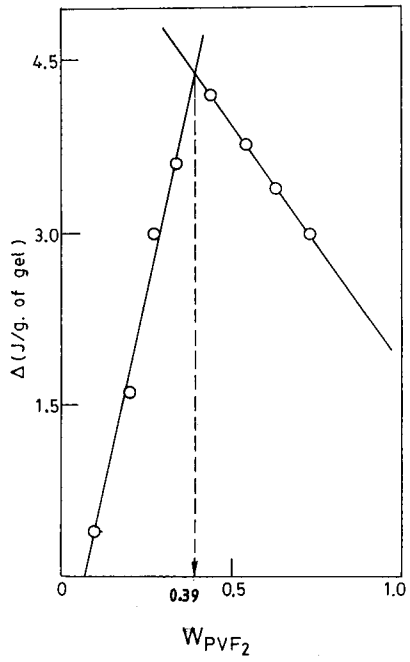

Figure 6. Deviation (Δ) vs the w_{PVF_2} plot of PVF_2/diethyl adipate gel.

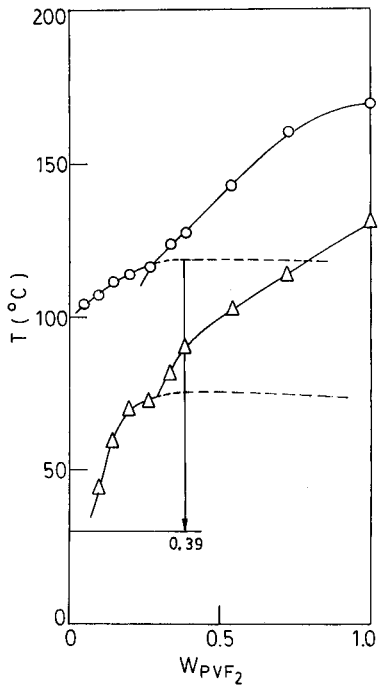

Figure 7. Gel-melting temperature and gelation temperature vs the w_{PVF_2} plot of PVF_2/diethyl adipate gel: ○, gel melting; △, gelation.

complex is not yet known. So from this analysis, it can be stated that this polymer−solvent complex formation inhibits the chain-folding process, yielding the fibrillar morphology of the gel.[29] A polymer chain passing through many such fibrils entrap the solvent to produce the gel. This is in sharp contrast to thermoreversible gelation of rodlike polymers where the end-to-end aggregation of the chain (enthalpic interaction) entraps the solvent to produce the gel.[30]

In Figure 7, the gel-melting (peak) temperature and the gelation peak temperature (obtained by dynamic cooling) are plotted with the blend composition. The nature of the plot is the same for both cases; however,

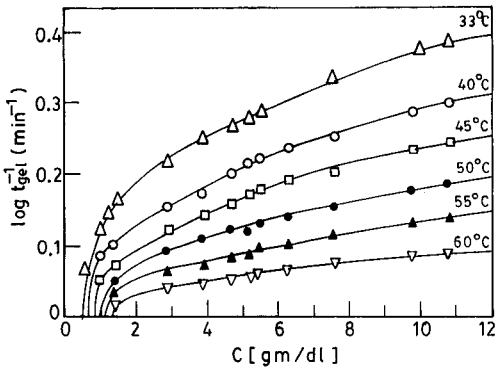

Figure 8. log t_{gel}^{-1} vs the concentration plot of PVF_2/diethyl adipate gel at the indicated temperatures.

there is a gap of about 40 °C between the plots and it is due to the hysteresis effect of the first-order phase-transition process.[7] The phase diagram of this system corresponds to the compound formation with an incongruent melting point.[24,26,31] The thermograms used in making the phase diagram have a single peak (endotherm or exotherm) and no separate peak for the compound is observed. So it may be considered that the melting endotherm is actually composed of two nondistinguishable peaks. The peak temperature of the first of these indistinguishable peaks is invariant with the concentration and it corresponds to

$$\text{compound} \rightarrow \text{liquid} + \text{solid} \tag{3}$$

and the second endotherm whose associated temperature is concentration-dependent corresponds to

$$\text{solid} \rightarrow \text{liquid} \tag{4}$$

In the figure the nonvariant transition is indicated by dotted lines as they are not directly detected in the DSC thermograms. Thus, the phase diagram also supports the formation of polymer−solvent complexes.

Kinetics of Gelation (Gelation Mechanism). Kinetics of gelation is an important tool to understand the gelation mechanism.[1−5] It can provide both the macroscopic and microscopic mechanism of gelation and this is usually done from the analysis of the gelation rate (t_{gel}^{-1}) which is usually expressed as a combination of two terms: the concentration term $f(C)$ and temperature function $f(T)$.[2,4,5,10]

$$t_{gel}^{-1} \propto f(C)f(T) \tag{5}$$

The gelation rate is usually considered as the inverse of the gelation time (t_{gel}^{-1}) which is measured by the test tube tilting method[1−5,10−12] for different polymer concentrations at different temperatures. In Figure 8 the gelation rate is plotted with the PVF_2 concentration at the indicated temperatures. The extrapolation of each curve to the zero gelation rate yields the critical gelation concentration ($C^*_{t=\alpha}$) which is an important parameter to analyze the gelation rate.[2,10]

The Concentration Function: Macroscopic Mechanism. An analysis of the concentration function of the rate expression usually yields the macroscopic mechanism of gelation.[5] At a fixed temperature

$$t_{gel}^{-1} \propto f(C) \tag{6}$$

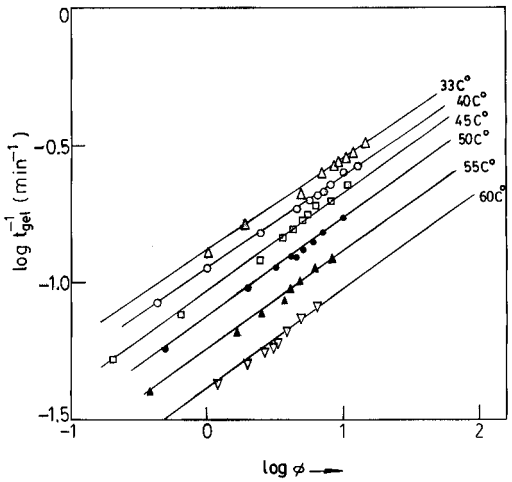

Figure 9. log t_{gel}^{-1} vs log ϕ plot of PVF_2/diethyl adipate gel at the indicated temperatures.

Table 2. C* and Exponent "*n*" Value for PVF_2–DEA Gels

T_{gel}, °C	C^*, g/dL	*n*
33	0.50	0.44
40	0.70	0.34
45	0.85	0.38
50	0.95	0.42
55	1.10	0.39
60	1.30	0.46
avg.		0.41
st. dev.		0.04

However, $f(C)$ is equal to ϕ^n, where ϕ is the reduced overlapping concentration:

$$\phi = [\{C - C^*_{t=\alpha}(T)\}/C^*_{t=\alpha}(T)]$$

and is analogous to the $p-p_c$ term of the percolation theory.[32,33] In Figure 9 the logarithmic plot of t_{gel}^{-1} and ϕ are shown and it is apparent from the figure that straight lines are obtained at each temperature. The *n* values are measured from the least-squares slope of each plot and are presented in Table 2. From the table it is clear that *n* values lie between 0.38 and 0.46. These values are very much close to β (0.45) for the percolation in a three-dimensional lattice.[32,33] Therefore, the present data lend support to the theory that the three-dimensional percolation is a suitable model for the gelation also in this system.[2,4,5]

The Temperature Function: Microscopic Mechanism. Analysis of the temperature coefficient of the gelation rate may provide a detailed molecular mechanism of gelation.[5] When the PVF_2 solution is cooled, it adopts an ordered TGT$\bar{G}$ conformation which is stabilized by a polymer–solvent complex formation, as discussed earlier. This ordered conformer then produces fibrillar crystals as evidenced from the SEM and TEM pictures of dried gel (Figure 1). The gelation process in this system can, therefore, be presented as

$$\text{coil} \rightarrow \text{TGT}\bar{\text{G}}\ \text{conformer} \rightarrow \alpha\text{-crystal (fibrillar gel)} \quad (7)$$

In the following sections we shall analyze the data of the gelation rate for both the processes.

Formation of the TGT$\bar{G}$ Conformer. The rate constant (K) for the transformation of the coil-to-TGT$\bar{G}$ conformer may be treated similarly to that of the coil-to-helix transition of a dilute aqueous collagen solution.[34]

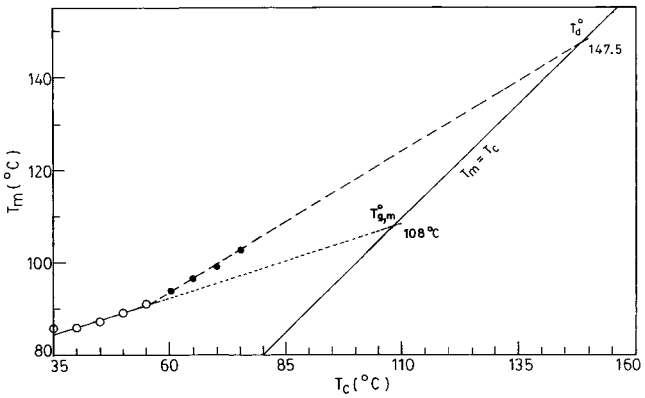

Figure 10. A representative Hoffman–Weeks plot of PVF_2/diethyl adipate gel (7.2 g/dL) to obtain the equilibrium gel-melting temperature (T_{gm}^0) and equilibrium dissolution temperature (T_d^0).

$$K = \text{const.}\ \exp(-A/kT\Delta T) \quad (8)$$

Since in the gelation process the first step is conformational ordering, at a particular concentration

$$t_{gel}^{-1} = \text{const.}\ \exp(-A/kT\Delta T_{gel}) \quad (9)$$

where $A = 2\sigma\Delta F/\Delta S$, σ is the surface energy arising due to the formation of a new surface in the ordered conformer, ΔF is the free energy of activation to produce the ordered conformer, and ΔS is the overall entropy change for the conformational ordering. $\Delta T_{gel} = T_{gm}^0 - T$, where T_{gm}^0 is the equilibrium gel-melting temperature. To obtain the T_{gm}^0, the Hoffman–Weeks[9] procedure is applied and a representative plot is shown in Figure 10. The gel-melting temperatures are determined by DSC at each gelation temperature for a fixed gelation time (3 h) in each case. As evidenced from Figure 8, above 60 °C no gelation rate could be measured because at those temperatures no gel is detected within a reasonable time period (24 h) but solution crystals are produced. So the Hoffman–Weeks plot of the solution crystals produced at higher temperatures are also presented in Figure 10; an extrapolation of this line to the $T_m = T_c$ line yields the equilibrium dissolution temperature (T_d^0). Thus, it is interesting to have two equilibrium melting temperatures (T_{gm}^0 and T_d^0) in the same system. The T_{gm}^0 represents the equilibrium temperature when the network structure breaks. Though crystals act as junction points, the equilibrium dissolution temperature is different from the equilibrium gel-melting temperature. This is because the critical gelation concentration (C^*) increases with an increase in T_c and at higher T_c; though crystals are produced, no gel is produced. In other words, the crystals which constitute the network structure are strained crystals and have much lower equilibrium melting than the solution crystals which are strain-free.

In Figure 11 plots of $\log(t_{gel}^{-1})$ versus $1/T\Delta T$ for three different concentrations of the solution are presented. The straight line nature of the plot supports the theory that conformational ordering is the first step in this process. From the least-squares slope values the values of ΔF are calculated using $\Delta S = \Delta H_u^0/C_\alpha$ [ΔH_u^0 = the enthalpy of fusion per repeating unit of PVF_2 (1.6 kcal/

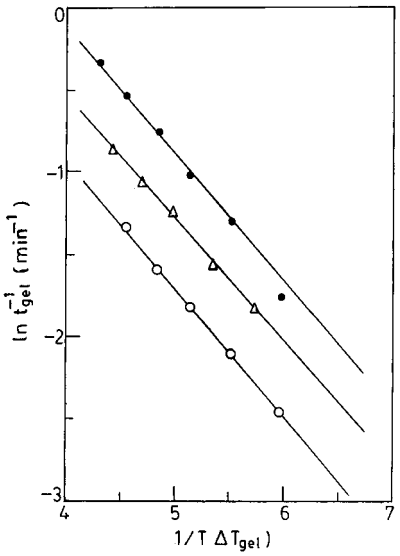

Figure 11. log t_{gel}^{-1} vs $1/T\Delta T_{gel}$ plot of PVF_2/diethyl adipate gel at three different concentrations: ●, 10.8 g/dL; △, 7.2 g/dL; ○, 4.7 g/dL.

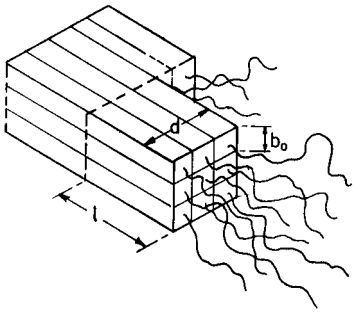

Figure 12. A model for the formation of fibrillar crystal from solution.

mol) and C_α is the chain characteristic ratio of PVF_2 (5.5)][35] and σ =1.38 kcal/mol[5] and are presented in Table 3. From the theoretical calculation of Farmer et al.[36] the potential energy (PE) barrier between the highest and lowest energy of the conformer is equal to 9 kcal/mol. Thus, the ΔF values presented in (Table 3) are almost in the same order as those with the theoretical PE barrier values.

Formation of Fibrillar Crystals in the Solution. In Figure 12 a model for fibrillar crystallization is presented.[37] The free energy of formation of the fibrillar nucleus of lateral dimension d and length l in the polymer melt may be expressed as

$$\Delta G = 4ld\sigma_s - d^2l\Delta g \qquad (10)$$

where σ_s is the surface energy of the fibrillar crystal and ΔG is the bulk free energy of the crystal per unit volume. In a polymer diluent mixture it can be expressed as

$$\Delta G_{dil} = 4ld\sigma_s - d^2l\Delta g - kT(d/b_0) \ln v_2 \qquad (11)$$

where the last term is an entropy contribution to the free energy arising because of the dilution of the crystallization unit by the diluent. v_2 is the volume fraction of the polymer, b_0 is the molecular width of the crystalline sequence, and $k \ln v_2^{(d/b_0)}$ indicate the probability of selecting a number of d/b_0 crystalline sequences of length l from the mixture.[38] Assuming the length l to be constant, the energy barrier for the formation of the fibrillar nucleus may be obtained by minimizing ΔG_{dil} with respect to d (i.e. $\delta\Delta G_{dil}/\delta d = 0$.[38,39] This yields the critical lateral dimension:

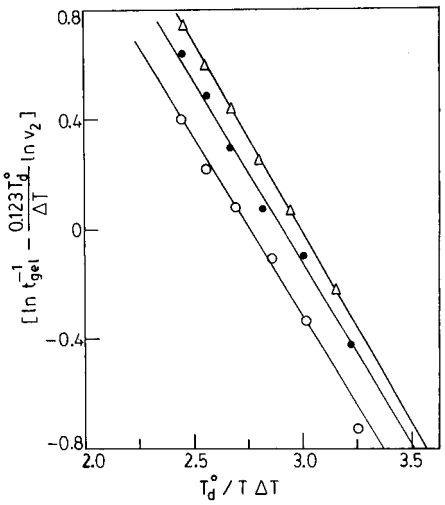

Figure 13. $(\ln t_{gel}^{-1} - 0.123T_d^0/\Delta T) \ln v_2$ vs $T_d^0/T\Delta T$ plot of PVF_2/diethyl adipate gel for indicated concentrations. △, 10.8 g/dL; ●, 7.2, g/dl; ○, 4.7, g/ dL.

$$d^* = 2\sigma_s/\Delta g - (kT/2b_0l\Delta g) \ln v_2 \qquad (12)$$

Putting the d^* in eq 11, the energy barrier for the formation of the fibrillar nucleus:

$$\Delta G_{dil}^* = 4l\sigma_s^2/\Delta g - (2\sigma_s kT/b_0\Delta g) \ln v_2 \qquad (13)$$

The bulk free energy of fusion (Δg) may be approximated to[40]

$$\Delta g = \Delta H_u^0 \Delta T/T_d^0$$

where ΔH_u^0 = the enthalpy of fusion per mole of the crystallizing unit and $\Delta T = T_d^0 - T$ where T_d^0 is the melting point of the crystalline phase in the mixture. Hence,

$$\Delta G_{dil}^* = 4l\sigma_s^2 T_d^0/\Delta H_u^0\Delta T - 2\,(\sigma_s kTT_d^0/b_0\,\Delta H_u^0\Delta T) \ln v_2 \qquad (14)$$

Using the Lauritzen−Hoffman expression,[40] the growth rate of fibrils can be written as

$$G = G_0 \exp[-G_a/kT] \exp[-4l\sigma_s^2 T_d^0/kT\Delta H_u^0\Delta T + (2\sigma_s T_d^0/b_0\Delta H_u^0\Delta T) \ln v_2]$$

Taking G = the gelation rate (t_{gel}^{-1}) and rearranging in logarithmic form

$$\ln t_{gel}^{-1} - (2\sigma_s T_d^0/b_0\Delta H_u^0\Delta T) \ln v_2 = A - 4l\sigma_s^2 T_d^0/kT\Delta H_u^0\Delta T \qquad (15)$$

where $A = \ln G_0 - G_a/KT$. Thus, a plot of the lhs of eq 15 with $T_d^0/T\Delta$T should yield a straight line. In Figure 13 plots are shown and in each case straight lines are observed. This indicates that the gelation rate is also proportional to the growth rate of the fibrillar crystal. Taking σ_s = 12.2 erg cm^{-2} [41] and $\Delta H_u^0 = 2.01 \times 10^9$ erg

Table 3. Kinetic Parameters for Conformational Changes and Crystallization Process of PVF_2−DEA Gels

conc., g/dL	T_{gm}^0, °C	A, kcal/mol	ΔF, kcal/mol	T_d^0, °C	l, Å	ΔG^*, kcal/mol
4.7	106	143.1	15.1	146	65	16.6
7.2	108	149.0	15.7	147.5	65	16.2
10.8	110	158.9	15.7	149.5	71	16.7

cm^{-3} [42] the length of the fibrils are calculated from the slopes and are presented in Table 3. It is about 65 Å and is almost constant with concentration.

It is now pertinent to calculate the energy barrier for fibrillar crystallization from eq 13 and these values are presented in the Table 3. It is apparent from the table that the energy barrier values for both the processes (conformational ordering and crystallization) are almost equal to each other. So it can be concluded that gel formation in this system is a concerted process, of conformational ordering and fibrillar crystallization.

Conclusion

From this study it may be concluded that PVF_2 gels in diethyl adipate producing α-phase PVF_2 crystals with a fibrillar morphology. The X-ray and FT-IR spectra indicate a solvated $TGT\bar{G}$ conformation of PVF_2 in the gel. The intensities of the X-ray diffraction peaks are mostly different from those of the melt-crystallized sample. The gels are transparent and thermodynamic study indicates polymer−solvent complexation which inhibits the chain folding. The phase diagram of this gel indicates compound formation with an incongruent melting point. Analysis of the kinetic data indicates that the gelation process obeys a three-dimensional percolation model.

The theory of fibrillar crystallization in the melt has been extended to a polymer solution and the gelation rate has been analyzed with this extended theory. The fibrillar length was found to be 65 Å, and from a comparison of the energy barrier values of the two processes it has been concluded that the gelation of this system is a concerted process, of conformational ordering and fibrillar crystallization.

References and Notes

(1) Cho, J. W.; Song, H. Y.; Kim, S. Y. *Polymer* **1993**, *34*, 1024.
(2) Mal, S.; Maiti, P.; Nandi, A. K. *Macromolecules* **1995**, *28*, 2371.
(3) Cho, J. W.; Lee, G. W. *J. Polym. Sci.* **1996**, *B34*, 1609.
(4) Mal, S.; Nandi, A. K. *Macromol. Symp.* **1997**, *114*, 251.
(5) Mal, S.; Nandi, A. K. *Polymer* **1998**, *39*, 6301.
(6) Lovinger, A. J. In *Developments in Crystalline Polymers−1*; Basset, D. C., Ed.; Elsevier Applied Science: London, 1981; p 195.
(7) Daniel, C.; Dammer, C.; Guenet, J. M. *Polymer* **1994**, *35*, 4243.
(8) Prest, W. M., Jr.; Luca, D. J. *J. Appl. Phys.* **1975**, *46*, 4238.
(9) Hoffman, J. D.; Weeks, J. J. *J. Res. Natl. Bur. Stand.* **1962**, *66*, 13.
(10) Ohkura, M.; Kaniaya, T.; Kaji, K. *Polymer* **1992**, *33*, 5044.
(11) Tan, H. M.; Hiltner, A.; Moet, A.; Baer, E. *Macromolecules* **1983**, *16*, 28.
(12) Prasad, A.; Mandelkern, L. *Macromolecules* **1990**, *23*, 5041.
(13) Lando, J. B.; Doll, W. W. *J. Macromol Sci. Phys.* **1968**, *2* (2), 205.
(14) Hasegawa, R.; Takahashi, Y.; Chatani, Y. *Polym. J.* **1972**, *3*, 600.
(15) Bachmann, M. A.; Lando, J. B. *Macromolecules* **1981**, *14*, 40.
(16) Datta, J.; Nandi, A. K. *Polymer* **1994**, *35*, 4804.
(17) Cortili, G.; Zebri, G. *Spectrochem. Acta* **1967**, *23A*, 2218.
(18) Enomoto, S.; Kawai, Y.; Sugita M. *J. Polym. Sci.* **1968**, *A26*, 861.
(19) Kobayashi, M.; Tashiro, K.; Tadokoro, H. *Macromolecules* **1975**, *8*, 158.
(20) Belke, R. E.; Cabasso, I. *Polymer* **1988**, *29*, 1831.
(21) Sundararajan, P. R.; Tyrer, N. J.; Bluhm, T. L. *Macromolecules* **1982**, *15*, 286.
(22) Daniel, Ch.; Deluca, M. D.; Guenet, J. M.; Brulet, A.; Menelle, A. *Polymer* **1996**, *37*, 127.
(23) Mal, S.; Nandi, A. K. *Langmuir* **1998**, *14*, 2238.
(24) Guenet, J. M.; Mckenna, G. B. *Macromolecules* **1988**, *21*, 1752.
(25) Spevacek, J.; Saini, A.; Guenet, J. M. *Macromol. Rapid Commun.* **1996**, *17*, 389.
(26) Guenet, J. M. *Thermochem. Acta* **1996**, *284*, 67.
(27) Ramazi, M.; Rochas, C.; Guenet, J. M. *Macromolecules* **1996**, *29*, 4668.
(28) Roerdink, E.; Challa, G. *Polymer* **1980**, *21*, 509.
(29) Guenet, J. M. *Macromolecules* **1987**, *20*, 2874.
(30) Tipton, D. L.; Russo, P. S. *Macromolecules* **1996**, *29*, 7402.
(31) Reisman, A. *Phase Equilibria*; Academic Press: New York, 1970.
(32) Stauffer, D.; Coniglio, A.; Adams, M. In *Advances in Polymer Science*; Dusek, K., Ed.; Springer-Verlag: Berlin, 1982; Vol. 44, p 108.
(33) Zallen, R. *The Physics of Amorphous Solids*; John Willey & Sons: New York, 1983; p 135.
(34) Flory, P. J.; Weaver, E. S. *J. Am. Chem. Soc.* **1960**, *82*, 4518.
(35) Hoffman, J. D.; Miller, R. L.; Marand, H.; Roitman, D. B. *Macromolecules* **1992**, *25*, 2221.
(36) Farmer, B. L.; Hopfinger, A. J.; Lando, J. B. *J. Appl. Phys.* **1972**, *11*, 4293.
(37) Pennings, A. J. *J. Polym Sci., Polym. Symp.* **1977**, *59*, 55.
(38) Boon, J.; Azcue, J. M. *J. Polym. Sci.* **1968**, *A-2* (6), 885.
(39) Godard, P.; Biebuyck, J. J.; Daumerie, M.; Naveau, H.; Mercier, J. P. *J. Polym. Sci., Polym. Phys. Ed.* **1978**, *16*, 1817.
(40) Hoffman, J. D.; Thomas Davis, G.; Lauritzen, J. I., Jr. In *Treatise on Solid State Chemistry, Vol. 3*; Hannay, N. B., Ed.; Plenum Press: New York, 1976; p 497.
(41) Datta, J.; Nandi, A. K. *Polymer* **1998**, *39*, 1921.
(42) Nakagawa, K.; Ishida, Y; *J. Polym. Sci.* **1973**, *B11*, 2153.

MA980764N